Angewandte Chemie
Eine Zeitschrift der Gesellschaft Deutscher Chemiker

Supporting Information

Key Intermediate Species Reveal the Copper(II)-Exchange Pathway in Biorelevant ATCUN/NTS Complexes

*Radosław Kotuniak, Marc J. F. Strampraad, Karolina Bossak-Ahmad, Urszula E. Wawrzyniak, Iwona Ufnalska, Peter-Leon Hagedoorn, and Wojciech Bal**

anie_202004264_sm_miscellaneous_information.pdf

Table of Contents

Materials and Methods 1
Spectroscopic parameters of Cu(II)-peptide complexes 2
Table S1........ 3
Table S2........ 3
Supplementary figures and tables 3
Figure S1.. 4
Figure S2.. 4
Figure S3.. 4
Figure S4. 5
Figure S5.. 5
Figure S6.. 6
Figure S7. 6
Figure S8.. 7
Table S3........ 7
Table S4........ 7
Figure S9. 8
Figure S10. 8
References........ 9

Materials and Methods

The Gly-Gly-His-OH peptide, $CuCl_2$, HCl, NaOH were purchased from Sigma. The MES (2-(N-morpholino)ethanesulfonic acid) and HEPES (4-(2-hydroxyethyl)-1-piperazineethanesulfonic acid) buffers were obtained from Carl Roth.

The UV−Vis experiments were performed at 25 °C in 1 cm-path-length quartz cuvettes (Hellma). The spectra were recorded using a Lambda 950 spectrophotometer (PerkinElmer) over the spectral range of 350 – 1000 nm. The control experiment of MES binding to Cu^{II} was performed using a solution of 10 mM $CuCl_2$ in 100 mM MES buffer (Fig. S1). In the pH-metric titration experiments (Fig. 2A), the GGH peptide was diluted in deionized water to 5 mM with the addition of $CuCl_2$ solution to obtain a 1:0.9 molar ratio. The solution was first acidified with HCl to pH = 1.7 and then titrated with small amounts of concentrated NaOH up to pH = 8.6. The pH in all experiments was controlled using an InLabMicro electrode calibrated daily with calibration buffers from Mettler-Toledo. The concentration-dependent experiment was carried out at pH = 4.5 set manually with HCl/NaOH in a water solution of Cu^{II}/GGH complex (Fig. 2B). The peptide concentration was varied from 0.5 to 70 mM, while keeping 1:0.9 peptide-to-metal molar ratio at each step. Based on the obtained absorbance intensity we selected the solution of 20 mM GGH and 18 mM $CuCl_2$ for temperature-dependent experiments performed in the range of 5 – 45 °C (Fig. S6).

Kinetic studies were performed at 25 °C using a SX20 stopped-flow spectrometer (Applied Photophysics Ltd.) and a 1 cm path length cuvette. Reactions were observed in the diode-array mode, with the spectra recorded in the 750 – 300 nm wavelength range at 0.66 ms intervals. The dead time of the instrument is 2 ms. Measurements were carried out for 4 mM GGH dissolved in 400 mM MES buffer at pH = 6.0, mixed with water solutions of $CuCl_2$ at concentrations from 1.2 to 3.6 mM (yielding 2 mM GGH with 0.6 – 1.8 mM Cu^{II} in the cuvette, due to the mixing dilution; Fig. 1). This concentration range was chosen to maintain the peptide excess over Cu^{II}, as otherwise the $Cu(OH)_2$ precipitation would disable the data analysis. For the same reason the source $CuCl_2$ solution was not buffered at pH = 6.0, but the high buffer concentration (400 mM) in the GGH solution stabilized the pH during the reaction. MES was selected as a non-coordinating buffer with respect to Cu^{2+} ions.[1] The SVD analysis and determination of rate constants were made using KinTek program.[2] Additional reactions at pH 7.0, 7.4 and 8.0 were recorded for a 3.2 mM $CuCl_2$ water solution and 4 mM GGH in 400 mM HEPES buffer (Fig. S5).

Microsecond freeze-hyperquenching (MHQ) experiments were performed by mixing (1:1) of 4 mM GGH peptide dissolved in 400 mM MES buffer at pH = 6.0 with 3.2 mM $CuCl_2$ in water. The reaction was stopped by freezing the mixture at different reaction times (100 µs to 1 s) on a cold rotating plate pre-cooled with liquid nitrogen. The reaction temperature was 9 ± 2 °C. The dead time of the instrument of 60 – 80 µs was included in the calculation of the reaction time. The frozen powder was collected in liquid nitrogen and stored at cryo-temperatures (77 K) until further analysis. The different reaction times were achieved by using a combination of the flow rate, the orifice of the mixing device and the distance of the mixer to the cold plate, as we described previously.[3] The MHQ frozen powder was packed into an EPR tube with a filter at the bottom. The tubes were kept in liquid nitrogen during and after packing to prevent continuation of the reaction.

The EPR spectra were measured with a Bruker EMXplus 9.5 EPR spectrometer at 40 K. The low temperature was maintained by boiling liquid helium and cold helium vapour was passed through a double-wall quartz glass tube, which was mounted and fitted in the rectangular cavity. The following experimental settings were used: microwave frequency, 9.405 GHz; microwave power, 2 mW (Fig. 3 and S7) and 0.4 mW (Fig. S8); modulation frequency, 100 kHz; modulation amplitude, 2.0 mT (Fig. 3 and S7) and 0.2 mT (Fig. S8).

The electrochemical experiments were performed using the CHI 1030 potentiostat (CH Instrument, Austin, USA) in a three-electrode arrangement with a silver/silver chloride (Ag/AgCl) as the reference, platinum wire as the counter and glassy carbon electrode (GCE, BASi, 3 mm diameter) as the working electrode. The reference electrode was separated from the working solution by an electrolytic bridge filled with 4 mM HNO_3/96 mM KNO_3. The potential of the reference electrode was calibrated by using the ruthenium electrode process in 100 mM KNO_3 solution, for which the formal potential (E_f) was – 175 mV. The GCE was sequentially mechanically polished with 1.0 and 0.3 µm alumina powders on a Buehler polishing cloth to a mirror-like surface, followed by 1 min water ultrasonication. All electrochemical measurements were carried out in 96 mM KNO_3 solutions containing 4 mM HNO_3 at pH 5.0 and 7.4. The pH was adjusted with submicroliter volumes of concentrated KOH or HNO_3 solutions. The pH was closely controlled before, during and at the end of each voltammetric measurement using a SevenCompact pH-meter (Mettler-Toledo) with an InLab Micro Pro micro combination pH electrode (Mettler-Toledo). The GGH concentrations were 0.5 or 1.0 mM. Much lower concentrations of GGH and Cu^{2+} ions used in all electrochemical measurements, compared to spectroscopic experiments were necessary to avoid the influence of unbound Cu^{2+} ions on the reduction of complexed Cu^{II}, which was impossible to completely eliminate otherwise. The ligand-to-Cu^{II} ratios were 1:0.9 and 2:0.9. For all presented CV curves, the scan rate (*v*) was 100 mV/s. Argon was applied to deaerate the solution and argon blanket was maintained over the solution during all experiments carried out at 22 °C.

Spectroscopic parameters of Cu(II)-peptide complexes

Equation S1 is the empirical formula proposed by H. Sigel and R. B. Martin for estimating the λ_{max} values in nm on the basis of the type of peptidic Cu^{II} ligands.[4] In the equation *n* refers to the number of specific interactions.

$$\lambda_{max} = \frac{10^3}{0.294 \times n_{C=O/H_2O} + 0.346 \times n_{COO^-} + 0.434 \times n_{Im} + 0.460 \times n_{NH_2} + 0.494 \times n_{N^-}} \quad \text{(S1)}$$

Supplementary figures and tables

Table S1. The λ_{max} and ε values for possible 1N, 2N, 3N and 4N complexes formed by Cu^{II} with GGH, based on the reference data for related peptides and Equation S1.

Coordination mode	Equation S1	Reference data		Reference
	λ_{max} (nm)	λ_{max} (nm)	ε (mol^{-1} cm^{-1})	
		1N		
N_{im}	760	740	21-27	[5]
NH_2	745	750 745-750	26 30	[6] [7]
		2N		
N_{im} + NH_2	**675**	**691-710**	**36 – 46**	[5]
N_{im} + N^-	660	Not available in the literature		
NH_2 + N^-	649	644-660 650 649	42-96 57 97	[7] [8] [9]
		3N		
N_{im} + N^- + NH_2	595	624	102	[5]
N_{im} + N^- + N^-	583	598 593 565 614	83 50 103 71	[5] [10] [11] [12]
NH_2 + N^- + N^-	574	540	153	[9]
		4N		
NH_2 + N^- + N^- + N_{im}	531	525	102	[13]

Table S2. Cu^{II} coordination/protonation patterns in Cu^{II}/GGH complexes possible theoretically in the pH range of 3.5-5.0.

Coordination mode	Stoichiometric formula	Comment
1N (N_{im} or NH_2)	CuH_2L	Protonated carboxyl
1N (N_{im} or NH_2)	CuHL	Deprotonated carboxyl
2N (N_{im} + NH_2)	CuHL	Protonated carboxyl
2N (N_{im} + NH_2)	CuL	Deprotonated carboxyl
2N (N_{im} or NH_2 + N^-)	CuL	Deprotonated carboxyl Protonated NH_2 or N_{im}
3N (N_{im} + N^- + NH_2)	CuL	Protonated carboxyl
3N (N_{im} + N^- + NH_2)	$CuH_{-1}L$	Deprotonated carboxyl
4N (N_{im} + N^- + N^- + NH_2)	$CuH_{-1}L$	Protonated carboxyl
4N (N_{im} + N^- + N^- + NH_2)	$CuH_{-2}L$	Deprotonated carboxyl

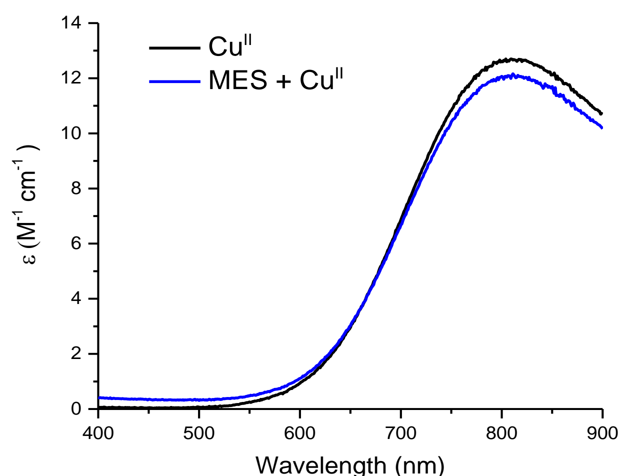

Figure S1. The reference spectra of the 97 mM $CuCl_2$ stock solution and 10 mM $CuCl_2$ in 100 mM MES.

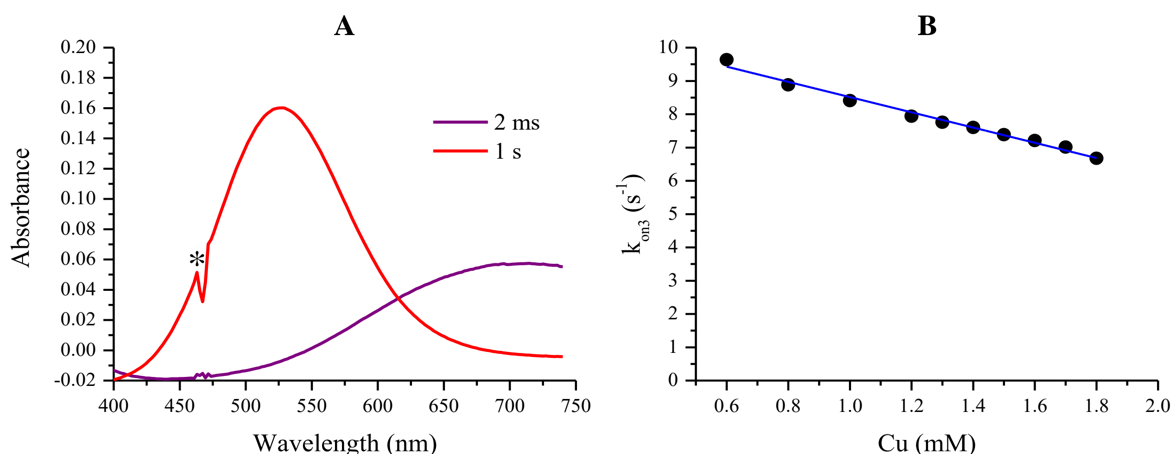

Figure S2. (A) Spectra recalculated using KinTek program for the stopped-flow experiment for 2 mM GGH peptide and 1.6 mM Cu^{II} at the beginning (purple) and the end (red) of the reaction. The spike at 470 nm is an instrumental artefact of the spectrophotometer. (B) Dependency of k_{on3} on Cu^{II} concentration in the presence of 2 mM GGH.*Spectrophotometer lamp artefact.

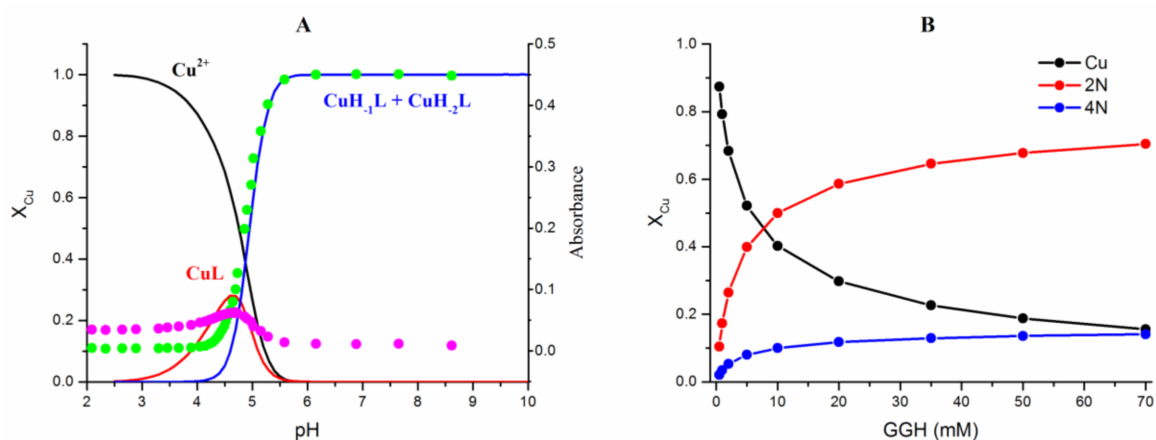

Figure S3. (A) The calculated species distribution diagram for 5 mM GGH and 4.5 mM Cu^{II} derived from potentiometry (solid lines) compared with UV-Vis absorption at 525 nm (green dots) and 705 nm (pink dots). (B) Simulation of distribution of 2N and 4N species for the concentration experiment (Fig. 2B) based on potentiometric results.[13]

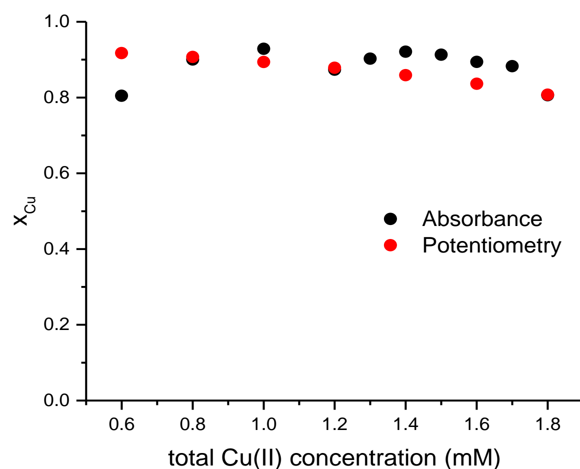

Figure S4. Molar fractions of the CuHL (2N) complex at pH = 6.0 of 2N band (calculated from absorbance intensity) recorded at the beginning of data collection (2 ms after mixing), comared with the theoretical abundance of this species in the absence of 4N complexes, calculated using potentiometry-derived stability constants for the concentrations of kinetic experiments: 2.0 mM GGH, 0.6 to 1.8 mM Cu^{II}.[13]

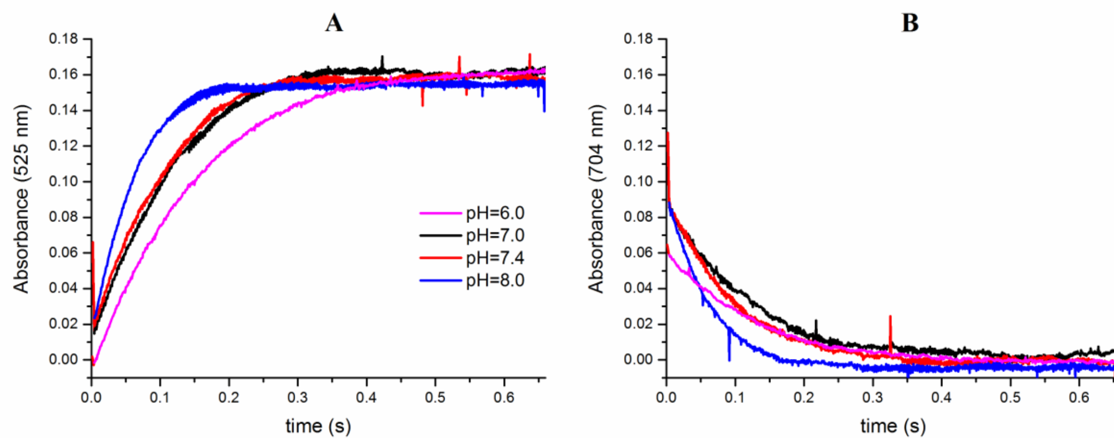

Figure S5. Stopped-flow kinetics traces for the formation of the Cu^{II}GGH 4N complex (A) and depletion of IC (B) at pH 6.0 (MES buffer), and 7.0, 7.4 and 8.0 (HEPES buffer). Final concentrations: 2.0 mM GGH, 1.8 mM Cu^{II}.

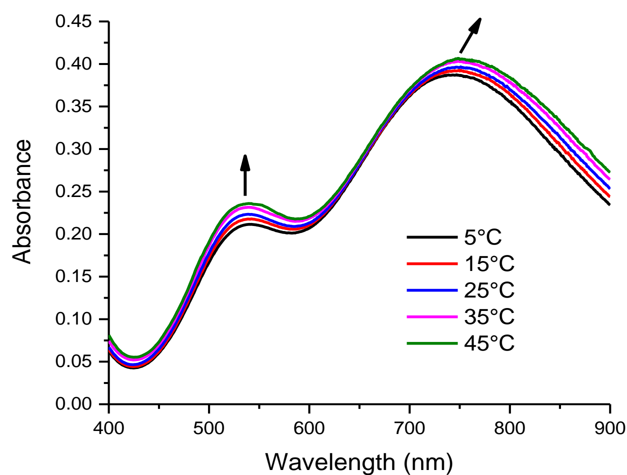

Figure S6. Temperature dependence of *d-d* bands in 18 mM Cu^{II} and 20 mM GGH solution at pH = 4.5 (determined at 25 °C and not corrected for temperature effects). Arrows mark directions of changes.

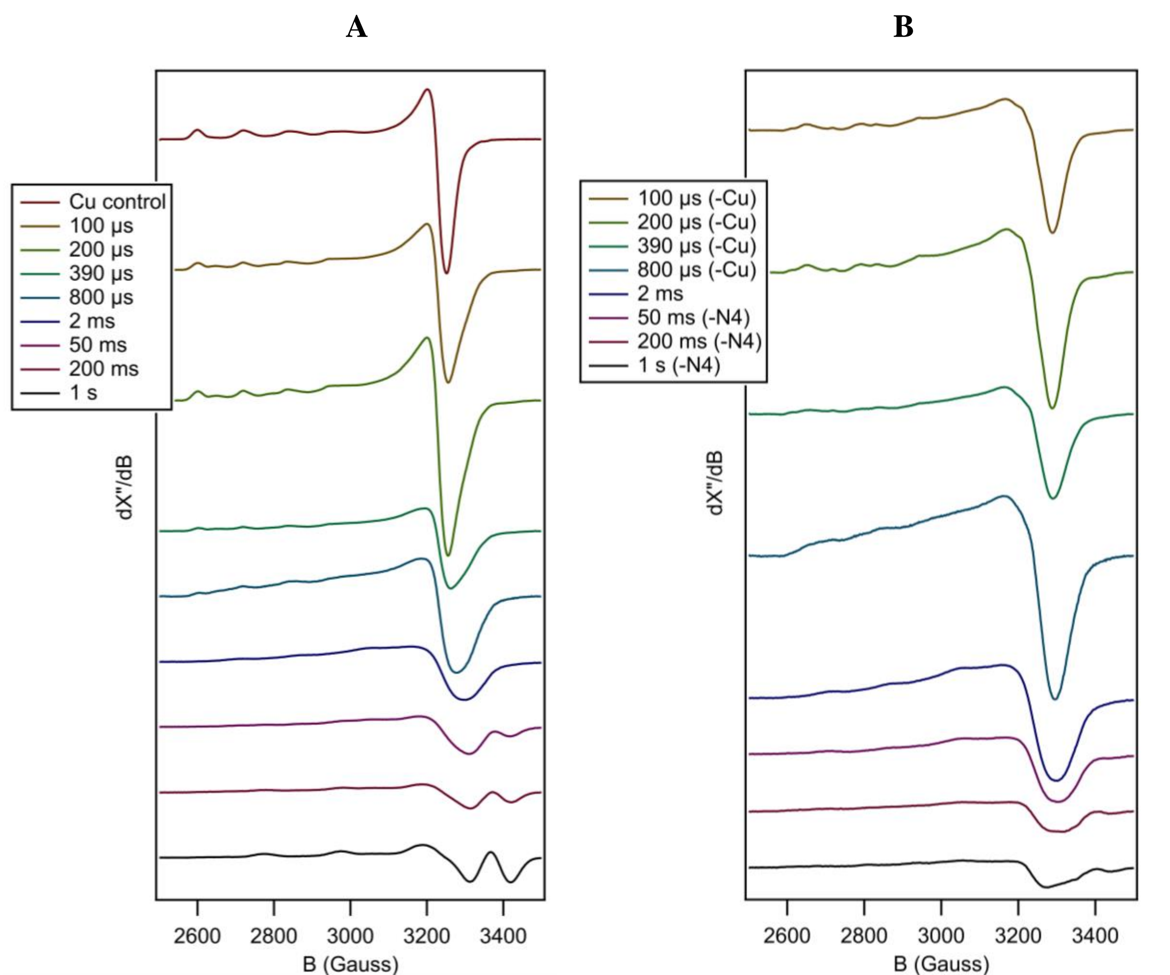

Figure S7. (A) Frozen solution EPR spectra obtained from reactions of 1.6 mM Cu^{II} with 2 mM GGH in 200 mM MES pH = 6.0 stopped by MHQ technique at indicated times. The EPR spectra (B) derived by subtraction of Cu^{II} control or the N4 complex control from (A) to highlight the intermediate spectra.

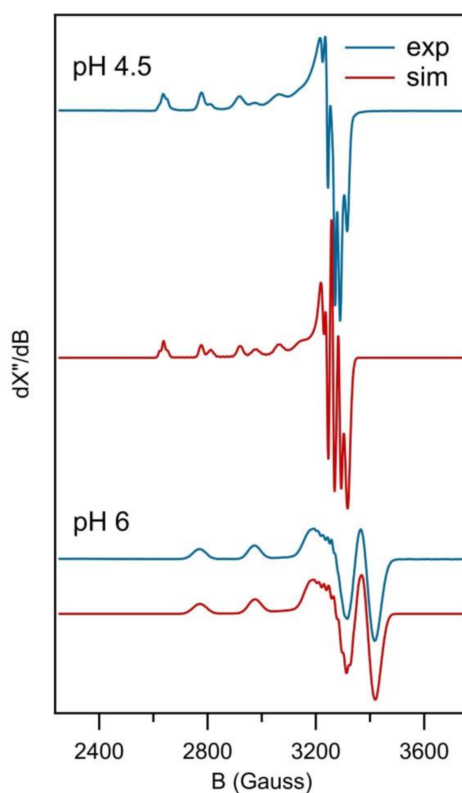

Figure S8. The experimental and simulated EPR spectra of complexes of 1.6 mM Cu^{II} and 2 mM GGH in 200 mM acetate buffer pH = 4.5 and 200 mM MES buffer pH = 6.0. Simulation parameters are provided in Table S4.

Table S3. EPR parameters of the MHQ sample spectra shown in Fig. 3.

Time (ms)	Main Component	g_{II}	A_{II} (Gauss)
0	Cu	2.470	120
0.2	EC	2.348	140
2	IC	2.259	156
1000	4N	2.184	203

Table S4. Simulation parameters for complexes of 1.6 mM Cu^{II} and 2 mM GGH in 200 mM acetate buffer pH=4.5 and 200 mM MES buffer pH=6.0.

pH	g_{xyz}	W_{xyz} (Gauss)	A_{xyz}–Cu (Gauss)	A_{xyz}–N4 (Gauss)	B_z
4.5	2.353, 2.063, 2.058	6, 10, 5	150, 10, 20	-	0.5
	2.316, 2.055, 2.054	8, 7, 10	173, 25, 25	-	0.5
6.0	2.181, 2.05, 2.035	12, 8, 10	213, 25, 20	12, 17, 13	0

Asymmetry parameter B_z defines a linewidth that varies with the metal nuclear orientation. Simulation program Hyperfine Spectrum (W.R. Hagen Visual software).[14]

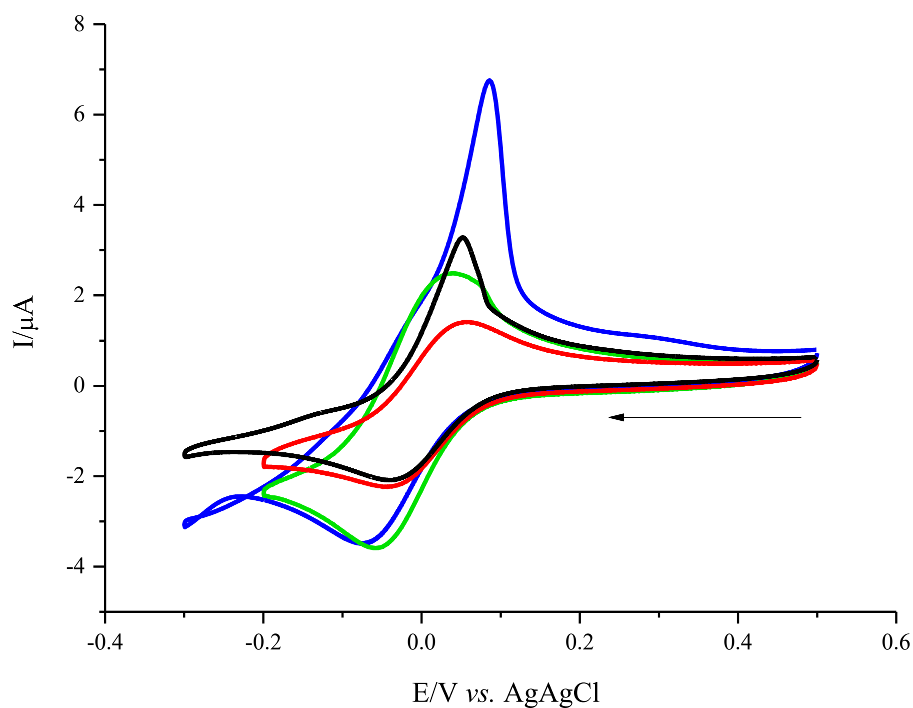

Figure S9. CVs for 0.45 mM Cu^{II} and 0.5 mM GGH (blue and green lines for scans initiated at 0.5 V terminated at -0.3 V and -0.2 V, respectively) and for 0.45 mM Cu^{II} and 1 mM GGH (black and red lines for scans initiated at 0.5 V and terminated at -0.3 and -0.2 V, respectively) in 96 mM KNO_3/ 4 mM HNO_3, pH 5.0. Red curve presents the electrochemical response specific for the 2N Cu^{II}/GGH complex. The arrow marks the direction of potential scan.

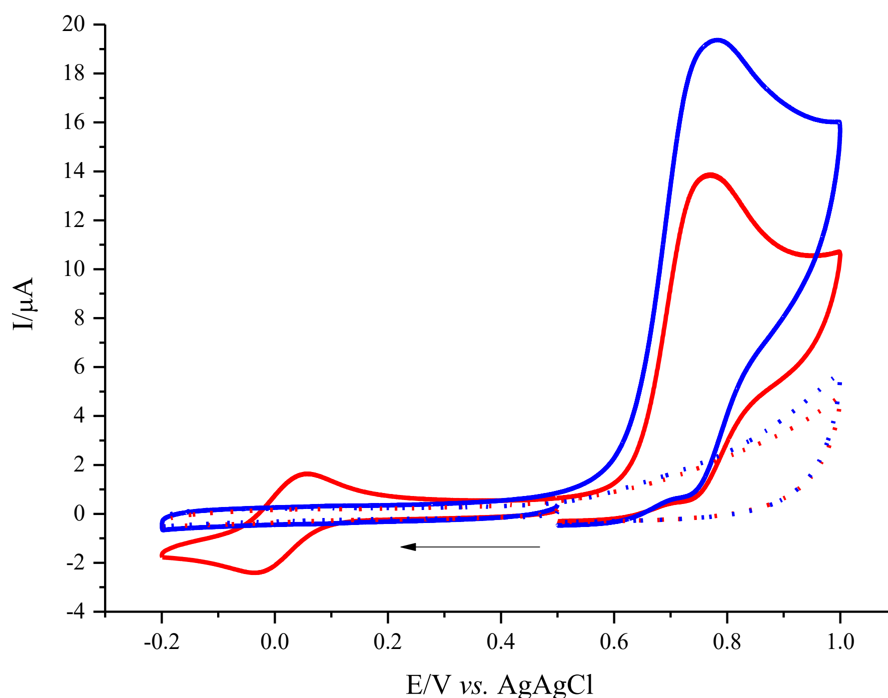

Figure S10. The comparison of CV curves recorded for 0.45 mM Cu^{II} and 1.0 mM GGH, in 96 mM KNO_3/4 mM HNO_3 at pH = 5.0 (red line) and pH = 7.4 (blue line). Dotted curves indicate experiments for 1.0 mM GGH alone at pH 5.0 (red) and 7.4 (blue), respectively. The scans were initiated and terminated at 0.5 V. The arrow marks the direction of potential scan.

References

[1] a) H. E. Mash, Y.-P. Chin, L. Sigg, R. Hari, H. Xue, *Analytical chemistry* **2003**, *75*, 671; b) N. E. Good, G. D. Winget, W. Winter, T. N. Connolly, S. Izawa, R. M. Singh, *Biochemistry* **1966**, *5*, 467.
[2] a) K. A. Johnson, Z. B. Simpson, T. Blom, *Anal. biochem.* **2009**, *387*, 20; b) K. A. Johnson, Z. B. Simpson, T. Blom, *Anal. biochem.* **2009**, *387*, 30.
[3] a) A. V. Cherepanov, S. de Vries, *Biochim. Biophys. Acta.* **2004**, *1656*, 1; b) B. Srour, M. J. F. Strampraad, W. R. Hagen, P.-L. Hagedoorn, *J. Inorg. Biochem.* **2018**, *184*, 42.
[4] H. Sigel, R. B. Martin, *Chem. Rev.* **1982**, *82*, 385.
[5] L. D. Pettit, S. Pyburn, W. Bal, H. Kozlowski, M. Bataille, *J. Chem. Soc., Dalton Trans.* **1990**, 3565.
[6] G. Formicka-Kozlowska, *J. Inorg. Biochem.* **1983**, *18*, 335.
[7] W. Bal, M. Dyba, F. Kasprzykowski, H. Kozłowski, R. Latajka, L. Łankiewicz, Z. Maćkiewicz, L. D. Pettit, *Inorg. Chim. Acta.* **1998**, *283*, 1.
[8] E. Lodyga-Chruscinska, G. Micera, E. Szajdzinska-Piêtek, G. Sanna, *J. Agric. Food Chem.* **1998**, *46*, 115.
[9] G. Formicka-Kozlowska, H. Kozlowski, B. Jezowska-Trzebiatowska, *Inorg. Chim. Acta.* **1977**, *25*, 1.
[10] A. Belczyk-Ciesielska, I. A. Zawisza, M. Mital, A. Bonna, W. Bal, *Inorg. Chem.* **2014**, *53*, 4639.
[11] K. Gerega, H. Kozlowski, E. Masiukiewicz, L. D. Pettit, S. Pyburn, B. Rzeszotarska, *J. Inorg. Biochem.* **1988**, *33*, 11.
[12] W. Bal, M. Jezowska-Bojczuk, H. Kozlowski, L. Chruscinski, G. Kupryszewski, B. Witczuk, *J. Inorg. Biochem.* **1995**, *57*, 235.
[13] K. Bossak-Ahmad, T. Frączyk, W. Bal, S. C. Drew, *ChemBioChem* **2020**, *21*, 331.
[14] W. R. Hagen, *Biomolecular EPR spectroscopy*, CRC Press, Boca Raton, **2008**.